



Published in final edited form as:

Nat Immunol. 2006 October ; 7(10): 1082–1091.

Transcription factors TFE3 and TFEB are critical for CD40 ligand expression and thymus-dependent humoral immunity

Chongmin Huan^{1,2}, Matthew L Kelly², Ryan Steele², Iuliana Shapira³, Susan R S Gottesman⁴, and Christopher A J Roman^{1,2}

¹ Program in Molecular and Cellular Biology, The School of Graduate Studies, New York, New York 11203, USA

² Department of Microbiology and Immunology and the Morse Institute for Molecular Genetics, New York, New York 11203, USA

³ Department of Medicine, Division of Hematology and Oncology, New York, New York 11203, USA

⁴ Department of Pathology, State University of New York, Downstate Medical Center at Brooklyn, New York, New York 11203, USA

Abstract

TFE3 and TFEB are broadly expressed transcription factors related to the transcription factor Mitf. Although they have been linked to cytokine signaling pathways in nonlymphoid cells, their function in T cells is unknown. TFE3-deficient mice are phenotypically normal, whereas TFEB deficiency causes early embryonic death. We now show that combined inactivation of TFE3 and TFEB in T cells resulted in a hyper-immunoglobulin M syndrome due to impaired expression of CD40 ligand by CD4⁺ T cells. Native TFE3 and TFEB bound to multiple cognate sites in the promoter of the gene encoding CD40 ligand (*Cd40lg*), and maximum *Cd40lg* promoter activity and gene expression required TFE3 or TFEB. Thus, TFE3 and TFEB are direct, physiological and mutually redundant activators of *Cd40lg* expression in activated CD4⁺ T cells critical for T cell-dependent antibody responses.

Transcription factors TFE3 and TFEB are the most closely related members of a functionally interactive DNA-binding family known as Mitf-TFE (MiT) that includes the microphthalmia-associated transcription factor Mitf and TFEB¹. MiT proteins bind to μ E3 sites, a subset of E-boxes that match a general CANNTG consensus sequence², with those binding to TFE3 *in vitro* first identified and characterized in immunoglobulin heavy-chain and T cell receptor (TCR) enhancers^{3–5}. DNA binding is mediated by nearly identical basic regions and requires homo- or heterodimer formation mediated by conserved helix-loop-helix and leucine zipper domains^{5–7}. Such interactions are restricted in the MiT family.

MiT proteins share similar structures and are often expressed together, yet genetic studies have demonstrated both overlapping and nonoverlapping functions for MiT proteins in different cell

Correspondence should be addressed to C.A.J.R. (christopher.roman@downstate.edu).

Note: Supplementary information is available on the Nature Immunology website.

AUTHOR CONTRIBUTIONS

C.H. and C.A.J.R. conceptualized and designed the research; C.H. created the TDN-transgenic mice and did most of the experimental work with the technical assistance of M.L.K.; R.S. did ELISAs with the assistance of C.H.; I.S. and S.R.S.G. prepared and analyzed spleen sections in conjunction with C.H.; C.A.J.R. and C.H. conceptualized and wrote the manuscript with input from S.R.S.G.; C.A.J.R. supervised the project.

COMPETING INTERESTS STATEMENT

The authors declare competing financial interests (see the *Nature Immunology* website for details).

types. Mitf, the most well characterized family member, is expressed mainly in pigment and myeloid cells, where it is involved in melanocyte and mast cell development^{8,9}. Mitf is an essential transcriptional mediator of the c-Kit pathway, which is critical for these cell lineages. Mice carrying a dominant negative allele of *Mitf* (*Mitf*^{Mi/Mi} mice) and mice with compound deficiency of Mitf and TFE3 also have defects in osteoclast development, because TFE3 and Mitf have overlapping and essential functions as transcriptional mediators of the macrophage colony-stimulating factor pathway^{10,11}. In addition, *Mitf*^{Mi/Mi} B cells show hyper-responsiveness and undergo a high frequency of spontaneous plasma cell differentiation¹², suggesting that Mitf acts as a negative regulator of B cell activation and terminal differentiation. Whether dominant negative interference with TFE3 and/or TFEB contribute to the *Mitf*^{Mi/Mi} B cell abnormality remains to be determined. *Mitf*^{Mi/Mi} T cells show no obvious defects in their development or function^{12,13}. Like expression of Mitf, TFEC expression is restricted mainly to the myeloid lineage¹⁴, but TFEC-deficient (*Tcfec*^{-/-}) mice are phenotypically normal, even though *Tcfec*^{-/-} macrophages have lower expression of a subset of interleukin 4 (IL-4)-responsive transcripts, including the transcript for granulocyte-macrophage colony-stimulating factor¹⁵.

Less understood are the individual physiological functions of TFE3 and TFEB, which are the most broadly expressed family members¹⁶. Studies of cultured nonlymphoid cell lines have indicated that TFE3 facilitates the activation of a subset of genes dependent on transcription factor Smad3, in response to transforming growth factor- β , including those encoding components of the extracellular matrix¹⁷. Ectopic overexpression of TFE3 in hepatocytes in mice promotes glycogen synthesis¹⁸. However, mice deficient in TFE3 (*Tcf3*^{-/-} mice) are phenotypically normal, with no defects noted in development, reproduction or the immune response¹¹ (K. Calame, personal communication). In contrast, *Tcf3*^{-/-} embryos die early in gestation because of defects in placental vascularization^{11,19}. The function of TFEB in the adult is not known.

Given the extensive amino acid sequence similarities and overlapping expression profiles, a possible explanation for the lack of a deleterious phenotype in *Tcf3*^{-/-} mice is that TFEB and TFE3 are functionally redundant in many tissues in which they are both expressed, where TFEB may compensate for TFE3 deficiency. In support of that idea, in cultured mesenchymal cells, native TFE3 and TFEB are mutually redundant transcription activators of the gene encoding E-cadherin²⁰. The idea that TFE3 and TFEB share any physiological functional redundancy *in vivo* has remained speculative. Using strategies to selectively inactivate these molecules in T cells, we demonstrate here a previously unknown, mutually redundant and central function for TFE3 and TFEB in humoral immunity through their control of expression of the gene encoding CD40 ligand (*Cd40lg*).

RESULTS

MiT inactivation in T cells causes hyper-IgM syndrome

We used immunoblot and RT-PCR analysis to assess the MiT expression profile in T cells. Of the four MiT proteins, we detected TFE3, TFEB and Mitf in total mouse thymocytes and resting splenic mouse CD4⁺ T cell extracts (Fig. 1a, **Supplementary Fig. 1** online and data not shown). After TCR stimulation of CD4⁺ T cells, the relative abundance of TFEB increased more than fivefold, whereas TFE3 remained constant. The increase in TFEB was at the post-transcriptional level, as relative amounts of steady-state *Tcf3* mRNA were unchanged (**Supplementary Fig. 1**). We detected a band that we interpreted to be the A isoform of Mitf in unstimulated CD4⁺ T cells, but did not detect it in TCR-stimulated cells (**Supplementary Fig. 1**). This corresponded to a decrease in Mitf mRNA (**Supplementary Fig. 1**). We did not detect TFEC expression in any of these samples by either immunoblot or RT-PCR (data not shown). In the human transformed T cell line Jurkat, both TFE3 and TFEB proteins were

present and their abundance did not change in response to pharmacological stimulation. We did not detect *Mitf* or *TFEC* in these cells (Fig. 1a, **Supplementary Fig. 1** and data not shown). Thus, in TCR-activated mouse $CD4^+$ T cells and Jurkat T cells, *TFE3* and *TFEB* were the only MiT family members expressed.

To study the functions of MiT proteins in T cells, we transgenically expressed an artificial *trans* dominant negative (TDN) protein in the T lineage. The TDN protein contains the *TFE3* helix-loop-helix-leucine zipper dimerization domains but lacks the DNA-binding basic region and transcription activation domains and thus forms inactive hetero-dimers with endogenous MiT proteins that are incapable of binding DNA²⁰. This strategy addressed any functional redundancies and the embryonic lethality of *TFEB* deficiency. We used an $E_{\mu}P_{\mu}$ transgene cassette²¹ to drive TDN protein expression in the lymphoid lineages (**Supplementary Fig. 2** online). As the expression profile of this transgene depends on the integration site²¹, we identified and analyzed lines expressing the TDN protein exclusively in the T cell lineage. In such T cell-specific lines, the TDN protein was expressed in thymocytes and splenic T cells but not in splenic or bone marrow B cells (Fig. 1b,c and **Supplementary Fig. 2**).

Analysis of lymphoid compartments in transgenic mice with T cell-specific TDN protein expression (called 'TDN-transgenic mice' here) indicated that B cell and T cell development was similar to that of nontransgenic mice in that the number and distribution of the predominant splenic B cell and T cell populations and thymocytes at 5 weeks of age were similar (Fig. 2). We then tested the immune competence of TDN-transgenic mice by evaluating their responses to the model T cell-dependent antigen sheep red blood cells (SRBCs). Comparison of spleen sections on days 8–9 after antigenic challenge showed that there was much less germinal center formation in TDN-transgenic mice than in their nontransgenic littermates. Most of the germinal centers, defined by the presence of peanut agglutinin (PNA)-binding germinal center B cells, were smaller and poorly formed in TDN-transgenic mice (Fig. 3a, left), even though $CD4^+$ T cells were present in the expected locations (Fig. 3a, middle). We confirmed the lower germinal center response by flow cytometry, which showed that the proportion of $CD19^+PNA^+$ splenic B cells in TDN-transgenic mice was one fourth that of their nontransgenic littermates (Fig. 3b).

Impaired germinal center formation is indicative of a lapse in T helper cell-dependent B cell activation and is predictive of impaired T cell-dependent antibody responses. Consistent with those data, serum titers of total immunoglobulin G (IgG) and IgA isotypes in naive TDN-transgenic mice were lower than those of their nontransgenic littermates, whereas total IgM concentrations were similar or slightly higher (Fig. 4a). We then directly tested the hypothesis of defective T cell help by evaluating the humoral responses of mice challenged with the T cell-independent and T cell-dependent antigens trinitrophenol-Ficoll (TNP-Ficoll) and trinitrophenol-keyhole limpet hemocyanin (TNP-KLH), respectively. TNP-specific IgM and IgG antibody responses to TNP-Ficoll were similar in TDN-transgenic and nontransgenic mice (Fig. 4b). However, the TNP-specific IgG response of TDN-transgenic mice to the T cell-dependent antigen TNP-KLH was much lower than that of their nontransgenic littermates at 14 and 21 d after immunization (Fig. 4c). Similarly, SRBC-specific plasma cell formation was also lower on a per-cell basis (Fig. 4d). Analysis of TDN-transgenic mice from two other independently generated T cell-specific lines also showed comparable T cell and B cell numbers and distribution but similarly impaired germinal center formation and generation of plasma cells in response to SRBC challenge compared with that of nontransgenic littermates (data not shown). In these ways, T cell-specific TDN-transgenic mice showed the hallmark phenotypes of hyper-IgM syndrome, in which antigen-independent lymphocyte development and antibody responses to T cell-independent antigens are intact, but germinal center formation and IgG responses to T cell-dependent antigens are defective²².

TFE3 and TFEB activate CD40 ligand expression

To better understand the basis for the humoral immune defect, we then assessed TDN-transgenic T cells by flow cytometry for their ability to express activation molecules important for effector functions of the germinal center response. The expression of CD40 ligand (CD40L) was much lower on the surface of TDN-transgenic CD4⁺ T cells than that of nontransgenic (wild-type) cells after TCR stimulation (Fig. 5a), whereas the induction of other molecules, including inducible costimulator (ICOS), CD25 and CD69, was indistinguishable (Fig. 5b,c and data not shown). CD28 expression and IL-4 secretion were also indistinguishable in nontransgenic versus TDN-transgenic T cells (Fig. 5d,e), and the growth of nontransgenic and TDN-transgenic T cells was also similar in the various culture conditions used in this study (data not shown). Impaired CD40L expression seemed to be at the transcriptional level, as real-time RT-PCR indicated a decrease in *Cd40lg* mRNA transcripts to one third that of nontransgenic cells at the induction peak (Fig. 5f). We obtained similar results with T cells from other independently generated, T cell-specific, TDN-transgenic lines (data not shown).

TFE3 and TFEB were the only MiT proteins detected in stimulated T cells that could be inhibited by the TDN protein and we thus inferred they were responsible for the impaired CD40L expression by TDN-transgenic T cells. The immune competence of *Tcfe3*^{-/-} mice further suggested that TFEB itself was necessary for CD40L expression or that TFE3 and TFEB were functionally redundant in this capacity. To test those hypotheses, we evaluated CD40L expression in primary wild-type and *Tcfe3*^{-/-} splenic CD4⁺ T cells rendered TFEB deficient by RNA-mediated interference achieved with lentiviral expression of small stem-loop RNA (siRNA)²⁰ (Supplementary Fig. 2). We infected T cells with a control lentivirus expressing only green fluorescent protein (GFP) or with a lentivirus expressing the TFEB siRNA and GFP, and cultured the cells with IL-2 (Fig. 5g). TCR-induced CD40L expression was similar in wild-type T cells infected with either the control or TFEB siRNA lentivirus and in *Tcfe3*^{-/-} T cells infected with the control lentivirus (Fig. 5g, top). These data confirmed published findings suggesting that immune functions of *Tcfe3*^{-/-} mice are intact, and furthermore suggested that TFEB itself was not essential if TFE3 were present. In contrast, induction of CD40L expression by *Tcfe3*^{-/-} T cells infected with the TFEB siRNA virus was substantially impaired compared with that of *Tcfe3*^{-/-} cells infected with the GFP-only control virus and wild-type cells. Induction of CD25 surface expression was unaffected by the TFEB siRNA in all cases (Fig. 5g, bottom). Growth of wild-type and *Tcfe3*^{-/-} T cells expressing TFEB siRNA was indistinguishable from that of uninfected cells and cells infected with the control GFP-only virus (data not shown). These results independently showed that TFE3 and TFEB have critical, direct and overlapping functions in the TCR-dependent induction of CD40L expression by primary CD4⁺ T cells. Our data also excluded the possibility that impaired CD40L expression was a secondary consequence of MiT-deficient T cell development or persistent TDN protein expression.

Defective CD40L expression underlies the hyper-IgM syndrome

Our findings suggested that defective CD40L expression by TDN-transgenic T cells was underlying the humoral immune defect in TDN-transgenic mice. Consistent with that, CD19⁺ B cells from TDN-transgenic mice and nontransgenic mice had similar expression of CD40 (Fig. 6a) and responded similarly to *in vitro* stimulation, including the CD40-dependent induction of CD86 and major histocompatibility complex (MHC) class II expression (Figs. 6b,c). Moreover, an agonist monoclonal antibody (mAb) to CD40, administered during immunization with TNP-KLH, enhanced day-7 TNP-specific IgG titers of both nontransgenic and TDN-transgenic mice, but most notably rendered the IgG responses indistinguishable from each other (Fig. 6d). In contrast, IgG antibody titers in mice treated with the isotype-matched control mAb were lower, and TDN-transgenic mice also had lower IgG responses than those of nontransgenic mice. These data indicated that B cell responses to T cell help and other

aspects of T cell help critical for this T cell-dependent antibody response were intact in the TDN-transgenic mice and supported the idea that the humoral immune defect in TDN-transgenic mice was T cell intrinsic and was due to defective CD40L expression.

TFE3 and TFEB directly activate *Cd40lg*

One mechanism by which TFE3 and TFEB could control CD40L expression is directly as transcription activators. Consistent with that model, we identified several E-box-like motifs in the promoters of the genes encoding human, mouse and rat CD40L, a subset of which matched known optimal μ E3-binding sites for MiT proteins² (**Supplementary Fig. 3** online). Some of these sites are reiterated and the configuration of many of these sites relative to ATG and to each other is conserved between species.

Chromatin immunoprecipitation assays showed that both endogenous TFE3 and TFEB bound to the *Cd40lg* promoter *in vivo*. Analysis of unstimulated and TCR-stimulated primary CD4⁺ splenic T cells from wild-type mice showed that TFE3 and TFEB each bound to a fragment of the mouse *Cd40lg* promoter in both resting and stimulated conditions (Fig. 7a, lanes 1, 2, 5 and 6, and **Supplementary Fig. 3**). We used the chromatin immunoprecipitation sample from *Tcfe3*^{-/-} cells with antibody to TFE3 (anti-TFE3) to define background band intensity; it was equivalent to that of the irrelevant antibody control (Fig. 7a, lanes 3 and 9). Whereas TFE3 binding did not change, TFEB binding increased after T cell activation by TCR crosslinking in a way that mirrored in the increase of TFEB protein abundance after TCR stimulation (Fig. 7a, lanes 5 and 6). The ability of TFEB to bind the fragment was independent of TFE3, as TFEB bound to the *Cd40lg* promoter in *Tcfe3*^{-/-} cells (Fig. 7a, lanes 6 and 7). We detected binding of neither TFE3 nor TFEB to the *Cd40lg* promoter by chromatin immunoprecipitation in TDN-transgenic CD4⁺ splenic T cells (Fig. 7a, lanes 4 and 8). Expression of TFE3 and TFEB proteins was indistinguishable in nontransgenic and TDN-transgenic T cells (**Supplementary Fig. 3**), further confirming the idea that endogenous TFE3 and TFEB DNA-binding activity was inactivated in those T cells by the transgenically expressed TDN protein.

Mobility-shift assays with nuclear extracts from primary CD4⁺ T cells established that native TFE3 and TFEB bound to the multiple MiT consensus E-boxes in the *Cd40lg* promoter, although to differing relative degrees and sometimes with 'preferential' binding of one or both subunits to individual sites (Fig. 7b). We obtained similar results by analyzing DNA-binding activities in extracts of HEK293 cells overexpressing TFE3 or TFEB (**Supplementary Fig. 3**). We demonstrated the specificity of the protein-DNA interactions by including TFE3- or TFEB-specific antibodies that interfered with DNA binding. In wild-type CD4⁺ T cells, native TFE3 and TFEB were immuno-precipitated together (**Supplementary Fig. 3**), suggesting that hetero-dimers can form and may represent a distinct DNA binding species. That interaction was blocked in TDN-transgenic T cells. In all cases, only basal binding activity was present in TDN-transgenic T cell extracts (Fig. 7b, bottom left). These data confirmed functional inactivation of endogenous TFE3 and TFEB by the transgenically expressed TDN.

To determine the importance of endogenous TFE3 and TFEB to *Cd40lg* promoter activity, we used a luciferase reporter gene assay. We linked mouse *Cd40lg* and human *CD40LG* promoter fragments to the gene encoding luciferase and transiently transfected these constructs into primary mouse CD4⁺ T cells and human Jurkat T cells. We compared the activity of 'full-length' promoters (spanning from the translational start site to about 1.5 kilobases upstream) containing the MiT consensus sites and truncated promoters lacking the MiT sites. We evaluated the contribution of endogenous TFE3 and TFEB to *Cd40lg* promoter activity by comparing promoter activity in the presence or absence of TDN protein. Transient transfection of the reporters into both primary mouse cells and transformed human cells demonstrated that the activity of the full-length mouse and human *Cd40lg* promoters was about threefold higher at the induction peak after T cell stimulation than that of the corresponding truncated promoters

lacking the consensus MiT binding sites (Fig. 8a, CD4⁺ T cells, 8 h after TCR stimulation; **Supplementary Fig. 4** online, Jurkat T cells, 20 h after pharmacological stimulation). However, simultaneous expression of the TDN protein, either by cotransfection or transgenic expression, reduced the activity of the full-length promoters to that of the truncated promoter fragments, whereas the activity of the truncated promoters was unaffected by TDN protein expression (Fig. 8a and **Supplementary Fig. 4**). Similarly, TDN protein expression selectively inhibited the induction of endogenous CD40L by Jurkat T cells dependent on phorbol myristate acetate (PMA) plus ionomycin, whereas the induction of CD25 was unaffected (**Supplementary Fig. 4**). The truncated promoters were still responsive to stimulation with anti-CD3 or PMA plus ionomycin, which we attributed to the proximal composite NFAT–AP-1 transcription factor recognition site, as has been reported^{23–25} (data not shown). Thus, deletion of an upstream DNA fragment of the mouse *Cd40lg* and human CD40LG promoters containing the predicted MiT consensus E-boxes rendered the promoters insensitive to endogenous TFE3 and TFEB, as demonstrated by the lack of an effect of the TDN protein. Therefore, endogenous TFE3 and/or TFEB were important for maximum induction of *Cd40lg* and *CD40LG* promoter activity in mouse and human T cells and seemed to have evolutionarily conserved functions in that capacity.

Point mutations that abrogated the binding of TFE3 and/or TFEB to individual sites also attenuated *Cd40lg* promoter activity in primary wild-type and *Tcfe3*^{-/-} CD4⁺ T cells (Fig. 8b), although to differing degrees. A full-length construct containing mutations of all eight sites had the greatest effect on promoter activity (Fig. 8b), reducing it to the activity of the truncated promoter. Individual mutation of sites three through seven had a less severe but measurably attenuating effects in both wild-type and *Tcfe3*^{-/-} T cells. In contrast, mutation of site one or two had no effect in wild-type cells but had a substantial effect in *Tcfe3*^{-/-} T cells. That result was consistent with the ‘preferential’ binding of TFEB from wild-type extracts to site one and the greater relative binding of TFEB to site two than to all other sites in the absence of TFE3 (Fig. 7b). The differential importance of some sites in *Tcfe3*^{-/-} versus wild-type cells may indicate that the TFE3 and TFEB redundancy was not complete or that sites had differential responsiveness to TFE3 or TFEB protein abundance. These results indicated that all sites in some context could act in concert for full TFE3- and/or TFEB-dependent enhancement of *Cd40lg* promoter activity. Thus, we infer that TFE3 or TFEB binding is critical for achieving the physiological regulation of CD40L expression necessary for T cell-dependent antibody responses.

DISCUSSION

Our studies here have demonstrated that TFE3 and TFEB are critical for T cell function and humoral immunity through their direct control of CD40L expression. As with the induction of many effector and activation molecules by T cell stimulation, such as IL-2 and TNF family members, CD40L induction is dependent on subunits of NFAT, a calcium-responsive transcription factor complex²⁶. Additional regulators include the AT-Hook transcription factor AKNA and subunits of transcription factors AP-1, NF-κB and Egr-1 (ref. 27), which are also shared by other TCR and/or costimulator-responsive genes. However, unlike those other genes, *Cd40lg* is the only one identified so far that requires TFE3 or TFEB. That requirement may contribute to the unique expression profile of *Cd40lg* compared with that of other TCR-responsive genes. Identifying the conditions and pathways that control TFE3 and TFEB activity will therefore be important in understanding the control of CD40L-dependent immunity and immunopathology.

In activated CD4⁺ T cells, TFE3 and TFEB were mutually redundant in controlling *Cd40lg* transcription, as a combined deficiency in TFE3 and TFEB inhibited TCR-dependent CD40L induction in the primary T cell culture systems, whereas individual deficiencies had a minor

or no effect. Thus, we have demonstrated physiological functional redundancy between TFE3 and TFEB *in vivo*, which may be a more general property of these proteins in other cell types. A degree of functional redundancy has also been reported among NFAT components in activating *Cd40lg* transcription, as a combined deficiency of NFATc1 and NFATc2 results in greater impairment in CD40L expression than does individual deficiency^{28,29}. However, it remains possible that in certain conditions, each has a unique contribution to the activation of *Cd40lg*. For example, only TFEB protein was induced after TCR stimulation of primary cells, most likely through post-transcriptional mechanisms, and TFEB bound to the *Cd40lg* promoter independently of TFE3. There were also differences in the relative importance of a subset of E-boxes to *Cd40lg* promoter activity in wild-type versus *Tcfe3*^{-/-} T cells. Those observations may indicate that there are physiological contexts in which TFEB or TFE3 may be more important, as has been proposed for NFAT subunits in T cell subsets³⁰ or in other cell types expressing CD40L^{31,32}.

The low, rather than absent, CD40L expression in activated T cells lacking TFE3 and TFEB activity is consistent with the limited degree of germinal center formation in TDN-transgenic mice, in contrast to that of mice with genetic *Cd40lg* deficiency, in which no germinal centers are found. We believe that the remaining CD40L expression was not due to incomplete inactivation of TFE3 and TFEB by the TDN protein, given that TDN protein expression inhibited the binding of endogenous TFE3 or TFEB to the *Cd40lg* promoter to basal binding amounts, as evaluated by electrophoretic mobility-shift assay and chromatin immunoprecipitation. It is possible that other μ E3 site-binding transcription factors not in the MiT family may bind to the promoter in their absence. These may include upstream stimulating factor and c-Myc, which are from distinct and noninteractive helix-loop-helix families^{6,33,34}. Upstream stimulating factor binds to a promoter target site normally occupied by TFE3 in *Tcfe3*^{-/-} but not wild-type fibroblasts³⁵. It has been suggested that c-Myc can also activate the *Cd40lg* promoter, but its effect is apparently indirect³⁶. Yet regardless of μ E3 site occupancy, we postulate that the absence of TFE3 and TFEB raises the activation threshold of the *Cd40lg* promoter by the remaining activators, such as NFAT and AP1. In that scenario, very large and sustained amounts of the other transcription activators, coupled with synergistic mechanisms such as mRNA and protein stabilization, could allow sufficient CD40L accumulation to overcome the TFE3 and TFEB deficiency in certain T cell clones highly activated by TCR, costimulators and interleukins.

The normal distribution of the main T cell populations in non-immunized TDN-transgenic mice suggested that other possible MiT target genes in T cells were not required for T cell development itself beyond the double-positive stage when the TDN protein was first detected. Those findings are consistent with the reported lack of developmental defects of *Mit*^{Mi/Mi} T cells¹² and indicate that TFE3 and TFEB are also not essential. Also unaffected were the expression of several TCR-responsive genes other than *Cd40lg* and antibody responses to the thymus-independent antigen. Those data suggest that MiT deficiency caused a relatively restricted T cell defect, in contrast to deficiencies in NFAT and NF- κ B subunits, which can radically affect T cell development, effector function or homeostasis^{37,38}.

Given those observations, we believe a deficit in CD40L expression is sufficient to account for the impaired T cell-dependent antibody responses noted in TDN-transgenic mice. Consistent with that, in some humans with X-linked hyper-IgM syndrome, the genetic defect leads to low rather than no or mutant CD40L expression³⁹. Nevertheless, our results do not rule out the importance of other putative TFE3 and TFEB target genes in T helper cell function not specifically addressed in our study here, or their importance in positive and negative selection. Although TFE3 has been directly and indirectly linked to several cytokine signaling pathways that control cell growth and differentiation in nonlymphoid cells, including c-Kit and transforming growth factor- β , cell type-specific and gene-specific regulation by each MiT

protein is an established characteristic of this family; pathway involvement established in one cell type cannot be directly extrapolated to other cell types and must be determined experimentally.

Many human diseases are associated with abnormal CD40L expression^{40,41}. For example, CD40L expression is often constitutively increased on T cells from patients with systemic lupus erythematosus and rheumatoid arthritis^{26,42,43}. In systemic lupus erythematosus, this occurs without abnormal expression of other markers of T cell activation. Transcriptional and post-transcriptional mechanisms that normally enhance CD40L expression are all thought to contribute to that phenomenon⁴². It has been shown that the Ras GTPase–mitogen-activated protein kinase (MAPK) pathway is necessary for the maintenance of abnormal CD40L expression by T cells from patients with systemic lupus erythematosus⁴⁴. Given that in non-lymphoid cells, TFE3 and TFEB can each be regulated by the Ras-MAPK pathway^{20,45,46}, a key issue will be whether the activity of TFE3 and TFEB can be regulated by MAPK activation in T cells (for example, in response to the TCR and IL-15 receptor) and if there are differences in their activity in normal versus autoimmune T cells. Moreover, given the broad distribution of TFE3 and TFEB expression in various cell types, it will be important to determine whether CD40L expression in other cell types, such as B cells, monocytes and platelets, depends on TFE3 and TFEB, and the effects of disease states on their expression in those cells. For example, B cell abnormalities in some autoimmune diseases may be due to homotypic stimulation through coexpression of CD40 and CD40L on abnormal B cells⁴¹. Future studies should determine whether TFE3 and TFEB, and/or pathways that influence their activity, are involved in the deregulated expression of CD40L in those clinical contexts and may be targets for intervention.

METHODS

Protein detection and coimmunoprecipitation

T cells were lysed in detergent buffer (150 mM NaCl, 20 mM Tris, pH 7.4, 1% (weight/volume) Triton X-100 and 0.1% (weight/volume) SDS), supplemented with Complete Protease Inhibitor tablets (Roche). Proteins were transferred to polyvinylidene difluoride membranes (Immobilon P). The following antibodies were used for immuno-blot analysis: anti-mouse TFE3 (mAb G138–312; BD-Pharmingen), anti-TFE3 (goat polyclonal; Santa Cruz Biotechnology), anti-TFEB (goat polyclonal; Abcam), anti-Mitf (mAb 21D1418; Abcam), anti-GAPDH (mAb 6C5; Chemicon), rabbit anti-goat IgG peroxidase conjugate (Sigma) and goat anti-mouse IgG peroxidase conjugate (Sigma). Blots were developed by enhanced chemiluminescence. Coimmunoprecipitation was done according to a protocol from BD-Pharmingen. Purified CD4⁺ splenocytes (2×10^7) were lysed in immunoprecipitation buffer (1% (weight/volume) Triton X-100, 150 mM NaCl, 10 mM Tris, pH 7.4, 1 mM EDTA, 1 mM EGTA, pH 8.0, 0.2 mM sodium orthovanadate, 0.5% (weight/volume) Igepal and protease inhibitor ‘cocktail’ (Roche)). Cell lysates were precleared with protein G–agarose beads (Roche) and then were incubated overnight with 5 μ g mAb to TFE3 (BD-Pharmingen). Immunoprecipitates were collected on protein G–agarose beads and were washed before elution in sample buffer for protein detection as described above.

Generation and identification of transgenic mice

Tcfe3^{-/-} mice¹¹ were provided by M. Ostrowski (Ohio State University, Columbus, Ohio). For the creation of TDN-transgenic mice, 3' hemagglutinin epitope–tagged TDN cDNA²⁰ was subcloned into an immunoglobulin heavy-chain gene enhancer and promoter–based transgene cassette (E_HP_H) that directs expression in T cells, B cells or both, depending on the line²¹ (a gift from J. Jacob, Emory University, Atlanta, Georgia; **Supplementary Fig. 2**). The excised transgene cassette was purified and was microinjected into fertilized FVB oocytes by standard

methods at the State University of New York–Downstate Transgenic Facility. Founder mice were identified by Southern blot and PCR of genomic DNA obtained by tail biopsy. Transgenic mice analyzed were the progeny of transgenic mice that had been back-crossed at least four generations onto the C57BL/6 strain. Ten independent lines were derived; five of those were confirmed as expressing the TDN transgene exclusively in the T lineage. All mice used were 5–6 weeks old and were hemizygous for the transgene; control mice were nontransgenic, sex-matched littermates of TDN-transgenic mice. The mice were housed in specific pathogen-free conditions in the Division of Laboratory Animal Resources of State University of New York–Downstate Medical Center and all experimental procedures were according to protocols approved by the Institutional Animal Care and Use Committee of the State University of New York–Downstate Medical Center (New York, New York).

Flow cytometry

For detection of cell surface markers, single-cell suspensions were treated with Fc receptor block (mAb 2–4G2; BD Pharmingen) and were stained with antibodies to CD19, B220, TCR β , CD40, CD40L, CD25, CD28, CD4, CD8, ICOS and/or CD86 conjugated to fluorescein isothiocyanate, phycoerythrin or CyChrome (BD Pharmingen) or with fluorescein isothiocyanate-conjugated anti-MHC class II (Caltag). For detection of the TDN protein in transgenic lymphocytes, cells were treated with the Fix & Perm kit (Caltag) before being stained with fluorescein isothiocyanate-conjugated anti-hemagglutinin (mAb 3F10; Roche). Cells were analyzed on a FACScan with CellQuest software (Benton Dickinson).

Immunocytochemical analysis of germinal centers

Mice were immunized intraperitoneally with 7.5 μ l SRBCs (Colorado Serum) in 200 μ l PBS. Spleens were collected 8 d after immunization and were fixed in 10% (weight/volume) formalin or were frozen with liquid nitrogen. For paraffin-embedded samples, germinal centers were stained as described⁴⁷ with modifications. ‘Antigen-retrieved’ slides were blocked using 3% (volume/volume) pig serum and an avidin-biotin blocking kit (Vector Lab), were incubated for more than 2 h with 1 μ g/ml of biotin-conjugated PNA (Sigma) and then were incubated for 45 min with biotin-conjugated goat anti-PNA (Vector Lab). Subsequently, sections were treated for 30 min with 0.1% (weight/volume) NaN₃ and 0.3% (volume/volume) H₂O₂ to block the endogenous peroxidase before being stained for 20 min with horseradish peroxidase-conjugated avidin diluted 1:400 (Dako). After being washed, sections were incubated for 20 min with horseradish peroxidase developing solution and then were embedded using glycerol gelatin. For frozen sections, germinal centers were stained with peroxidase-conjugated PNA (Sigma), biotin-conjugated anti-CD4 (RM4–5; BD Pharmingen) and anti-B220 (RA3-6B2; BD Pharmingen) as described⁴⁸.

Enzyme-linked immunosorbent assay (ELISA) and immunization

Total serum titers of IgM, IgG1, IgG2a, IgG2b, IgG3 and IgA were determined with mouse ELISA quantification kits (Bethyl Lab). Bound immunoglobulin was detected with a tetramethylbenzidine peroxidase substrate system (KPL). The T cell-independent type II and T cell-dependent immunizations and immune response assays were done as described⁴⁹. *In vivo* stimulation of B cells with mAb to CD40 was done as described⁴⁸ with modifications. Mice were immunized intraperitoneally with 100 μ g TNP-KLH (Biosearch Technologies) in complete Freund’s adjuvant (Difco) and were injected intravenously each day for 7 d after immunization with 100 μ g anti-CD40 (mAb 3/23; BD Pharmingen) or the isotype control rat IgG2a κ (mAb R35–95; BD Pharmingen), and then blood was collected to obtain serum. Serum immunoglobulin specific for TNP was measured using Immulux HB plates (DYNEX) coated with TNP-BSA (Biosearch Technologies) with ELISA quantification kits (Bethyl Lab). An EL405 auto plate washer (Bio-Tek) was used for ELISA; plates were ‘read’ at 450 nm with a

μ Quant microplate spectrophotometer (Bio-Tek) and data were analyzed with KC Junior microplate data analysis software (Bio-Tek). For IL-4 analysis, the cytokine content of T cell culture supernatants was assayed with the Mouse IL-4 Immunoassay ELISA kit (R&D) following the manufacturer's protocol.

Plaque-forming cells

The spleen IgM anti-SRBC response was assayed 5 d after intraperitoneal administration of 0.5–7.5 μ l SRBCs in 200 μ l PBS following the protocol of the Jerne plaque assay⁵⁰.

Cell culture

For CD4⁺ T cell purification and T cell activation, CD4⁺ T cells were purified from the spleens of 5-week-old mice with a mouse CD4 Negative Isolation kit (DynaL Biotech) to a purity of 96% or more, as determined by flow cytometry. Jurkat T cells were provided by K. Alexandropoulos (Columbia University, New York, New York). T cells were cultured in RPMI medium supplemented with 10% (volume/volume) heat-inactivated FCS (Gibco) and 50 μ M β -mercaptoethanol (Sigma). For the lentiviral siRNA experiment, 20 units/ml of mouse IL-2 (Roche) was added to the culture medium. For TCR stimulation, purified mouse splenic CD4⁺ T cells, either cultured in IL-2 for 4–5 d (siRNA) or freshly isolated, were incubated for approximately 8 h in plates coated with 5–10 μ g/ml of anti-CD3 ϵ (mAb 145-2C11; BD Pharmingen) before being collected for the detection of surface CD40L and CD25 expression. For CD28 expression, cells were incubated with or without 10 μ g/ml of anti-CD3 for 48 h after initiation of the culture as described⁵¹. For ICOS expression analysis, T cells were incubated for 48 h with 10 μ g/ml of anti-CD3 following the manufacturer's instructions (BD Pharmingen). IL-4 cytokine analysis was done as described²⁸; CD4⁺ T cells were removed from anti-CD3 stimulation after 48 h, were cultured for 7 d in supplemented RPMI medium containing 100 units/ml of mouse IL-2 (Roche), then were restimulated for 48 h at a density of 1×10^5 cells/well in 96-well plates coated with 5 μ g/ml of plate-bound anti-CD3 without IL-2. Supernatants were collected for quantitative ELISA. For real-time RT-PCR, freshly isolated and purified splenic CD4⁺ T cells were incubated for 0 h, 3 h, 6 h and 9 h in supplemented RPMI medium in plates coated with 10 μ g/ml of plate-bound anti-CD3 before cells were collected for RNA extraction and reverse transcription. For stimulation of Jurkat cells, PMA (final concentration, 20 ng/ml) and ionomycin (final concentration, 1.5 μ M) were added to the supplemented RPMI culture medium for 12 or 24 h before cells were collected for fluorescent antibody staining and reporter gene assays, respectively.

For B cell purification and B cell stimulation, splenic B cells were purified with a mouse B cell Negative Isolation kit (DynaL Biotech) such that 94% or more of the cells were CD19⁺. Purified B cells were then analyzed directly for CD40 expression or were stimulated for 48 h with mAb to CD40 (3/23; BD Pharmingen) as described⁵² and then were analyzed for CD86 and MHC class II surface expression by flow cytometry.

RT-PCR and real-time RT-PCR

Total RNA from approximately 2×10^7 purified CD4⁺ splenic T cells were analyzed per time point for real-time RT-PCR. RNA was isolated with TRI reagent (MART) and contaminant DNA was removed by DNase I (Sigma) according to the manufacturer's instructions. Total RNA (5 μ g) was reverse-transcribed and amplified by PCR with the QuantiTect SYBR Green RT-PCR kit (Qiagen) in an Opticon Continuous Fluorescence Detector (MJ Research). The relative abundance of mouse *Cd40lg* and glyceraldehyde phosphate dehydrogenase (*Gapdh*) mRNA was measured by real-time RT-PCR with the following primers: for *Cd40lg*, 5'-AAAATGGGAAA CAGCTGACG-3' and 5'-GGTATTTGCCGCCTTGAGTA-3'; for *Gapdh*, 5'-TC ACCACCATGGAGAAGGC-3' and 5'-GCTAAGCAGTTGGTGGTGCA-3'. The abundance of *Cd40lg* mRNA was normalized to that of *Gapdh* mRNA. RT-PCR was done

as described²⁰. Oligonucleotides to detect *Tcfe3*, *Tcfcb*, *Tcfec*, *Mitf* and *Gapdh* cDNA by RT-PCR have been described^{14,20}.

Lentivirus-delivered siRNA

The control and TFEB siRNA lentiviruses have been described²⁰, and viral particles were produced according to published protocols⁵³. The siRNA targeting *Tcfcb* mRNA was inserted into the pLentiLox 3.7 plasmid, which was transfected into 293 cells together with the packaging vectors pMDLg/pRRE, CMV-VSVG and RSV-Rev (provided by E. Brown, University of Pennsylvania, Philadelphia, Pennsylvania). Viruses in the culture media were concentrated by centrifugation and were used to infect purified mouse spleen CD4⁺ T cells. Infected T cells were cultured for 4–5 d with 20 units/ml of IL-2 before infection efficiency and anti-CD3 responses were evaluated.

Chromatin immunoprecipitation

These assays were done as described²⁰ with the following modifications. Purified mouse spleen CD4⁺ T cells (1.5×10^7), left unstimulated or stimulated for 8 h with anti-CD3, were used for immunoprecipitation with 5 µg of the following antibodies: anti-TFE3 (mAb G138-312; BD Pharmingen), anti-TFEB (polyclonal; Abcam) and anti-GAPDH (mAb 6C5; Chemicon). Then, 10% of the precipitated DNA and 0.11% of the input DNA were used as templates for each PCR consisting of 29 cycles of 1 min at 94 °C, 1 min at 61 °C and 1.5 min at 72 °C. PCR products were separated by 5% PAGE. Primers for amplification of the mouse *Cd40lg* promoter region were 5'-CACAGACAGCATCCCTAGCA-3' (forward) and 5'-CTAAGCTGAGGCCAAACCAC-3' (reverse).

Electrophoretic mobility-shift assay

These assays were done as described⁵⁴ with the following modifications. Nuclear extracts from anti-CD3-activated CD4⁺ T cells or transfected HEK293 cells (5 µg) were incubated on ice for 30 min with a ³²P-labeled oligonucleotide spanning an E-box site from the mouse *Cd40lg* promoter (**Supplementary Table 1** online) in 25 mM HEPES, pH 7.9, 50 mM KCl, 4% (weight/volume) Ficoll, 5 µM ZnCl₂, 0.1 mM dithiothreitol, 0.02% (volume/volume) Nonidet-P40, 5 mM MgCl₂, 10 µg/ml of BSA and 10 ng/µl of poly(dI:dC). Nonspecific binding was assessed in the presence of a 100-fold excess of unlabeled oligonucleotide corresponding to the labeled oligonucleotide with or without E-box mutation (**Supplementary Table 1**) and 2.5 µg anti-TFE3 (BD-Pharmingen) or anti-TFEB (Santa Cruz). Samples with antibody were incubated for additional 30 min. Reaction products were separated by native 5% (weight/volume) PAGE at 4 °C and were visualized by autoradiography.

Cd40lg promoter reporter gene assays

The 5' extended (full-length; to positions –1535 base pairs and –1562 base pairs relative to mouse and human ATG, respectively) and truncated mouse *Cd40lg* and human *CD40LG* promoter fragments (to positions –382 base pairs and –944 base pairs from ATG, respectively) were amplified from genomic DNA by PCR and were inserted into the pGL3 luciferase reporter vector (Promega). Mouse *Cd40lg* promoter reporter gene plasmids with E-box mutations (CANNTG to CTNNTG) were constructed by site-directed mutagenesis (Stratagene) with specific primers (**Supplementary Table 2** online). Jurkat cells were transfected by electroporation with 10 µg of *Cd40lg* or *CD40LG* promoter reporter gene plasmids, 50 ng of the control reporter Renilla reniformis luciferase (RLuc) and 8 µg of empty pEBB (control) or pEBB-TDN expression vector and were then activated with PMA and ionomycin as described²³. Firefly luciferase and RLuc activity was measured in cell extracts with the Dual Luciferase Reporter Assay system (Promega) and a TD-20/20 luminometer (Turner Designs). Primary mouse CD4 T cells were transfected with 2.5 µg of *Cd40lg* promoter reporter gene

plasmid, 0.01 μg of RLuc and 1.5 μg of empty pEBB or pEBB-TDN expression plasmid for each sample using the mouse T cell Nucleofector kit (Amaxa). Then, 2 d after transfection, the cells were activated for 8 h with 5 $\mu\text{g}/\text{ml}$ of mAb to CD3 ϵ and then were lysed for luminometry as described above. Luciferase activity was always normalized to RLuc activity. In all experiments, the total amount of pEBB expression vector DNA was made equivalent with an empty pEBB plasmid. Mean normalized luciferase values \pm s.e.m. were calculated and plotted on bar graphs.

Acknowledgements

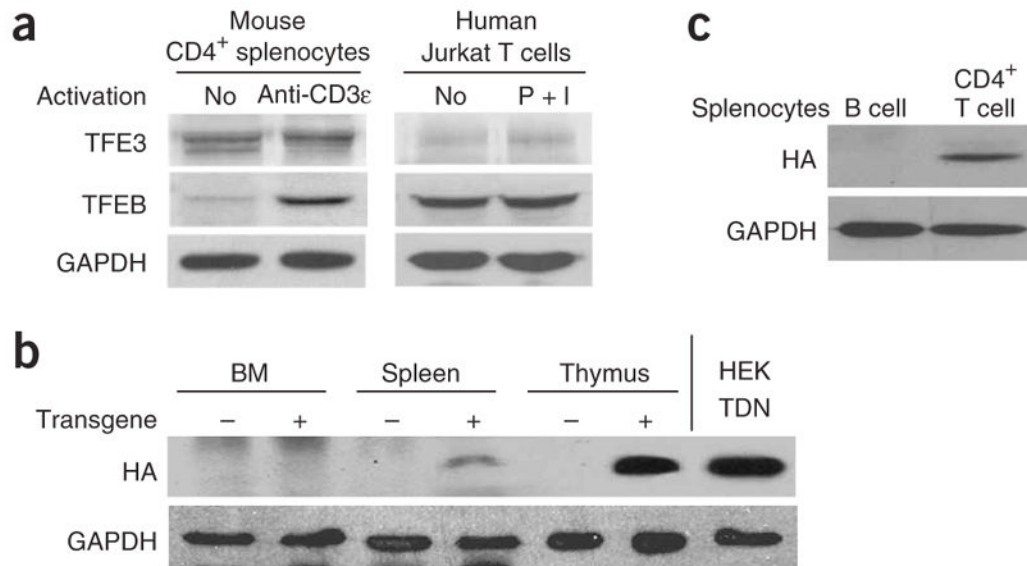
We thank L. Braithwaite-Harte and S. Mirra (Department of Pathology, State University of New York, Downstate Medical Center at Brooklyn) for sharing expertise and reagents for histology; H. Siddiqi (Department of Microbiology and Immunology, State University of New York, Downstate Medical Center at Brooklyn) for help in establishing ELISAs; O. Ramadan for technical assistance in mouse genotyping; K. Calame (Columbia University, New York, New York) for sharing unpublished results and discussions; K. Alexandropoulos (Columbia University, New York, New York), W. Pear (University of Pennsylvania, Philadelphia, Pennsylvania) and A. Pernis (Columbia University New York, New York) for critical reading of the manuscript, advice and discussions; and P. Cortes and lab members (Mount Sinai School of Medicine, New York, New York) for providing access to their laboratory for primary T cell transfection studies. Supported by the Dean's Initiative Pilot Project (State University of New York, Downstate Medical Center; C.A.J.R.) and the National Institutes of Health (DK65011 to C.A.J.R.).

References

1. Steingrimsson E, Copeland NG, Jenkins NA. Melanocytes and the microphthalmia transcription factor network. *Annu Rev Genet* 2004;38:365–411. [PubMed: 15568981]
2. Aksan I, Goding CR. Targeting the microphthalmia basic helix-loop-helix-leucine zipper transcription factor to a subset of E-box elements *in vitro* and *in vivo*. *Mol Cell Biol* 1998;18:6930–6938. [PubMed: 9819381]
3. Beckmann H, Su LK, Kadesch T. TFE3: a helix-loop-helix protein that activates transcription through the immunoglobulin enhancer muE3 motif. *Genes Dev* 1990;4:167–179. [PubMed: 2338243]
4. Roman C, Cohn L, Calame K. A dominant negative form of transcription activator mTFE3 created by differential splicing. *Science* 1991;254:94–97. [PubMed: 1840705]
5. Roman C, et al. mTFE3, an X-linked transcriptional activator containing basic helix-loop-helix and zipper domains, utilizes the zipper to stabilize both DNA binding and multimerization. *Mol Cell Biol* 1992;12:817–827. [PubMed: 1732746]
6. Beckmann H, Kadesch T. The leucine zipper of TFE3 dictates helix-loop-helix dimerization specificity. *Genes Dev* 1991;5:1057–1066. [PubMed: 2044953]
7. Rehli M, Den Elzen N, Cassady AI, Ostrowski MC, Hume DA. Cloning and characterization of the murine genes for bHLH-ZIP transcription factors TFEC and TFEB reveal a common gene organization for all MiT subfamily members. *Genomics* 1999;56:111–120. [PubMed: 10036191]
8. Fisher DE. Microphthalmia: a signal responsive transcriptional regulator in development. *Pigment Cell Res* 2000;13(Suppl 8):145–149. [PubMed: 11041373]
9. Tachibana M. MITF: a stream flowing for pigment cells. *Pigment Cell Res* 2000;13:230–240. [PubMed: 10952390]
10. Hershey CL, Fisher DE. Mitf and Tfe3: members of a b-HLH-ZIP transcription factor family essential for osteoclast development and function. *Bone* 2004;34:689–696. [PubMed: 15050900]
11. Steingrimsson E, et al. Mitf and Tfe3, two members of the Mitf-Tfe family of bHLH-Zip transcription factors, have important but functionally redundant roles in osteoclast development. *Proc Natl Acad Sci USA* 2002;99:4477–4482. [PubMed: 11930005]
12. Lin L, Gerth AJ, Peng SL. Active inhibition of plasma cell development in resting B Cells by microphthalmia-associated transcription factor. *J Exp Med* 2004;200:115–122. [PubMed: 15226356]
13. Roundy K, Kollhoff A, Eichwald EJ, Weis JJ, Weis JH. Microphthalmic mice display a B cell deficiency similar to that seen for mast and NK cells. *J Immunol* 1999;163:6671–6678. [PubMed: 10586063]

14. Rehli M, Lichanska A, Cassady AI, Ostrowski MC, Hume DA. TFEC is a macrophage-restricted member of the microphthalmia-TFE subfamily of basic helix-loop-helix leucine zipper transcription factors. *J Immunol* 1999;162:1559–1565. [PubMed: 9973413]
15. Rehli M, et al. Transcription factor Tfec contributes to the IL-4-inducible expression of a small group of genes in mouse macrophages including the granulocyte colony-stimulating factor receptor. *J Immunol* 2005;174:7111–7122. [PubMed: 15908341]
16. Kuiper RP, Schepens M, Thijssen J, Schoenmakers EF, van Kessel AG. Regulation of the MiTF/TFE bHLH-LZ transcription factors through restricted spatial expression and alternative splicing of functional domains. *Nucleic Acids Res* 2004;32:2315–2322. [PubMed: 15118077]
17. Hua X, Liu X, Ansari DO, Lodish HF. Synergistic cooperation of TFE3 and smad proteins in TGF- β -induced transcription of the plasminogen activator inhibitor-1 gene. *Genes Dev* 1998;12:3084–3095. [PubMed: 9765209]
18. Nakagawa Y, et al. TFE3 transcriptionally activates hepatic IRS-2, participates in insulin signaling and ameliorates diabetes. *Nat Med* 2006;12:107–113. [PubMed: 16327801]
19. Steingrimsson E, Tessarollo L, Reid SW, Jenkins NA, Copeland NG. The bHLH-Zip transcription factor Tfeb is essential for placental vascularization. *Development* 1998;125:4607–4616. [PubMed: 9806910]
20. Huan C, Sashital D, Hailemariam T, Kelly ML, Roman CAJ. Renal carcinoma associated transcription factors TFE3 and TFEB are leukemia-inhibitory factor-responsive transcription activators of E-cadherin. *J Biol Chem* 2005;280:30225–30235. [PubMed: 15994295]
21. Tepper RI, et al. IL-4 induces allergic-like inflammatory disease and alters T cell development in transgenic mice. *Cell* 1990;62:457–467. [PubMed: 2116236]
22. Durandy A, Peron S, Fischer A. Hyper-IgM syndromes. *Curr Opin Rheumatol* 2006;18:369–376. [PubMed: 16763457]
23. Lobo FM, Xu S, Lee C, Fuleihan RL. Transcriptional activity of the distal CD40 ligand promoter. *Biochem Biophys Res Commun* 2000;279:245–250. [PubMed: 11112447]
24. Lindgren H, Axcrone K, Leanderson T. Regulation of transcriptional activity of the murine CD40 ligand promoter in response to signals through TCR and the costimulatory molecules CD28 and CD2. *J Immunol* 2001;166:4578–4585. [PubMed: 11254715]
25. Parra E, Mustelin T, Dohlsten M, Mercola D. Identification of a CD28 response element in the CD40 ligand promoter. *J Immunol* 2001;166:2437–2443. [PubMed: 11160303]
26. Cron RQ. CD154 transcriptional regulation in primary human CD4 T cells. *Immunol Res* 2003;27:185–202. [PubMed: 12857968]
27. Cron RQ, et al. Early growth response-1 is required for CD154 transcription. *J Immunol* 2006;176:811–818. [PubMed: 16393964]
28. Peng SL, Gerth AJ, Ranger AM, Glimcher LH. NFATc1 and NFATc2 together control both T and B cell activation and differentiation. *Immunity* 2001;14:13–20. [PubMed: 11163226]
29. Hodge MR, et al. Hyperproliferation and dysregulation of IL-4 expression in NF-ATp-deficient mice. *Immunity* 1996;4:397–405. [PubMed: 8612134]
30. Harris NL, et al. Nuclear factor of activated T (NFAT) cells activity within CD4⁺ T cells is influenced by activation status and tissue localisation. *Microbes Infect* 2006;8:232–237. [PubMed: 16203169]
31. Imadome K, Shirakata M, Shimizu N, Nonoyama S, Yamanashi Y. CD40 ligand is a critical effector of Epstein-Barr virus in host cell survival and transformation. *Proc Natl Acad Sci USA* 2003;100:7836–7840. [PubMed: 12805559]
32. Mach F, et al. Functional CD40 ligand is expressed on human vascular endothelial cells, smooth muscle cells, and macrophages: implications for CD40–CD40 ligand signaling in atherosclerosis. *Proc Natl Acad Sci USA* 1997;94:1931–1936. [PubMed: 9050882]
33. Kerkhoff E, Bister K, Klempnauer KH. Sequence-specific DNA binding by Myc proteins. *Proc Natl Acad Sci USA* 1991;88:4323–4327. [PubMed: 1827916]
34. Fisher DE, Parent LA, Sharp PA. Myc/Max and other helix-loop-helix/leucine zipper proteins bend DNA toward the minor groove. *Proc Natl Acad Sci USA* 1992;89:11779–11783. [PubMed: 1465398]
35. Giangrande PH, Zhu W, Rempel RE, Laakso N, Nevins JR. Combinatorial gene control involving E2F and E Box family members. *EMBO J* 2004;23:1336–1347. [PubMed: 15014447]

36. Skov S, et al. Histone deacetylase inhibitors: a new class of immunosuppressors targeting a novel signal pathway essential for CD154 expression. *Blood* 2003;101:1430–1438. [PubMed: 12393479]
37. Macian F. NFAT proteins: key regulators of T-cell development and function. *Nat Rev Immunol* 2005;5:472–484. [PubMed: 15928679]
38. Siebenlist U, Brown K, Claudio E. Control of lymphocyte development by nuclear factor- κ B. *Nat Rev Immunol* 2005;5:435–445. [PubMed: 15905862]
39. Seyama K, et al. Mutations of the CD40 ligand gene and its effect on CD40 ligand expression in patients with X-linked hyper IgM syndrome. *Blood* 1998;92:2421–2434. [PubMed: 9746782]
40. Danese S, Fiocchi C. Platelet activation and the CD40/CD40 ligand pathway: mechanisms and implications for human disease. *Crit Rev Immunol* 2005;25:103–121. [PubMed: 15952932]
41. Schattner EJ. CD40 ligand in CLL pathogenesis and therapy. *Leuk Lymphoma* 2000;37:461–472. [PubMed: 11042507]
42. Crow MK, Kirou KA. Regulation of CD40 ligand expression in systemic lupus erythematosus. *Curr Opin Rheumatol* 2001;13:361–369. [PubMed: 11604589]
43. Toubi E, Shoenfeld Y. The role of CD40–CD154 interactions in autoimmunity and the benefit of disrupting this pathway. *Autoimmunity* 2004;37:457–464. [PubMed: 15621572]
44. Yi Y, McNERney M, Datta SK. Regulatory defects in Cbl and mitogen-activated protein kinase (extracellular signal-related kinase) pathways cause persistent hyper-expression of CD40 ligand in human lupus T cells. *J Immunol* 2000;165:6627–6634. [PubMed: 11086108]
45. Hemesath TJ, Price ER, Takemoto C, Badalian T, Fisher DE. MAP kinase links the transcription factor microphthalmia to c-Kit signalling in melanocytes. *Nature* 1998;391:298–301. [PubMed: 9440696]
46. Weilbaecher KN, et al. Linkage of M-CSF signaling to Mitf, TFE3, and the osteoclast defect in *Mitf^{mi/mi}* mice. *Mol Cell* 2001;8:749–758. [PubMed: 11684011]
47. Cattoretti G, et al. BCL-6 protein is expressed in germinal-center B cells. *Blood* 1995;86:45–53. [PubMed: 7795255]
48. McAdam AJ, et al. ICOS is critical for CD40-mediated antibody class switching. *Nature* 2001;409:102–105. [PubMed: 11343122]
49. Yamazaki T, et al. Essential immunoregulatory role for BCAP in B cell development and function. *J Exp Med* 2002;195:535–545. [PubMed: 11877477]
50. Jerne NK, et al. Plaque forming cells: methodology and theory. *Transplant Rev* 1974;18:130–191. [PubMed: 4615402]
51. Gross JA, Callas E, Allison JP. Identification and distribution of the costimulatory receptor CD28 in the mouse. *J Immunol* 1992;149:380–388. [PubMed: 1320641]
52. Hasbold J, Johnson-Leger C, Atkins CJ, Clark EA, Klaus GG. Properties of mouse CD40: cellular distribution of CD40 and B cell activation by monoclonal anti-mouse CD40 antibodies. *Eur J Immunol* 1994;24:1835–1842. [PubMed: 7519998]
53. Rubinson DA, et al. A lentivirus-based system to functionally silence genes in primary mammalian cells, stem cells and transgenic mice by RNA interference. *Nat Genet* 2003;33:401–406. [PubMed: 12590264]
54. Slomiany BA, Kelly MM, Kurtz DT. Extraction of nuclear proteins with increased DNA binding activity. *Biotechniques* 2000;28:938–942. [PubMed: 10818701]

**Figure 1.**

TFE3 and TFEB expression in T cells and TDN protein expression in TDN-transgenic mice. **(a)** Immunoblot of TFE3 and TFEB in primary CD4⁺ mouse splenocytes and Jurkat T cells. CD4⁺ splenic T cells were stimulated for 8 h by incubation with mAb to CD3 (Anti-CD3ε); Jurkat T cells were stimulated for 20 h with PMA plus ionomycin (P+I). An extended time course is presented in **Supplementary Fig. 1**. Data are representative of at least three independent experiments. **(b,c)** Expression profiles of TDN protein in TDN-transgenic mice. **(b)** Immunoblot of extracts from total bone marrow (BM), total spleen (Spleen) and total thymocytes (Thymus) from TDN-transgenic mice (+) and nontransgenic littermates (-). HEK TDN, total extracts of HEK293 cells transfected with a plasmid expressing TDN cDNA. **(c)** Immunoblot of extracts of purified splenic B cells and CD4⁺ T cells from TDN-transgenic mice. HA, hemagglutinin. GAPDH, loading control. Data are representative of at least three independent experiments.

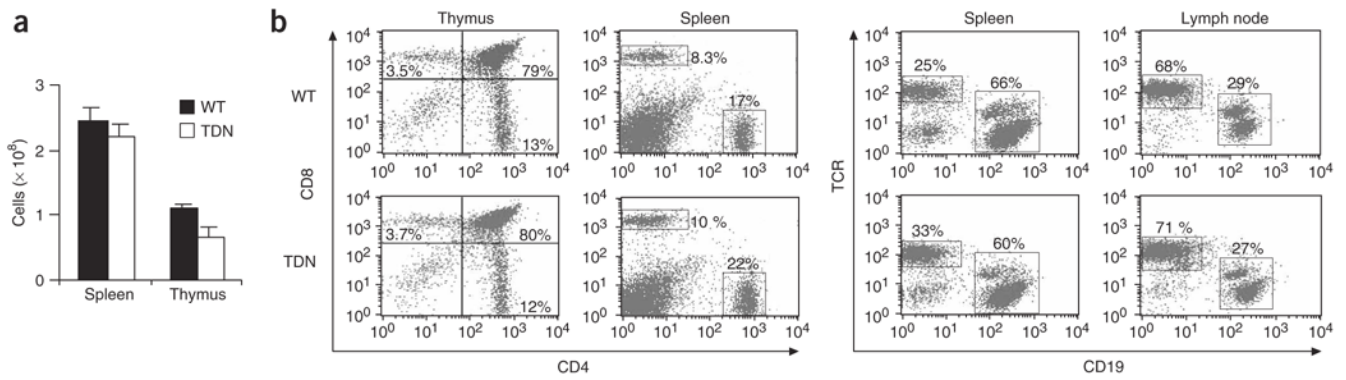


Figure 2.

Distribution of the predominant B cell and T cell populations in TDN-transgenic mice. Cells from the primary and secondary lymphocyte compartments of 5- to 6-week-old mice were analyzed. **(a)** Total splenocytes and thymocytes. Error bars, s.e.m.; $n = 6$ transgenic (TDN) and nontransgenic (WT) sex-matched littermate pairs. **(b)** Flow cytometry of lymphocyte-gated mononuclear cells from various lymphoid organs (above plots) for markers specific for particular developmental stages and subsets. Numbers in quadrants or beside boxed areas indicate percent cells in each. Data are representative of at least six independent analyses.

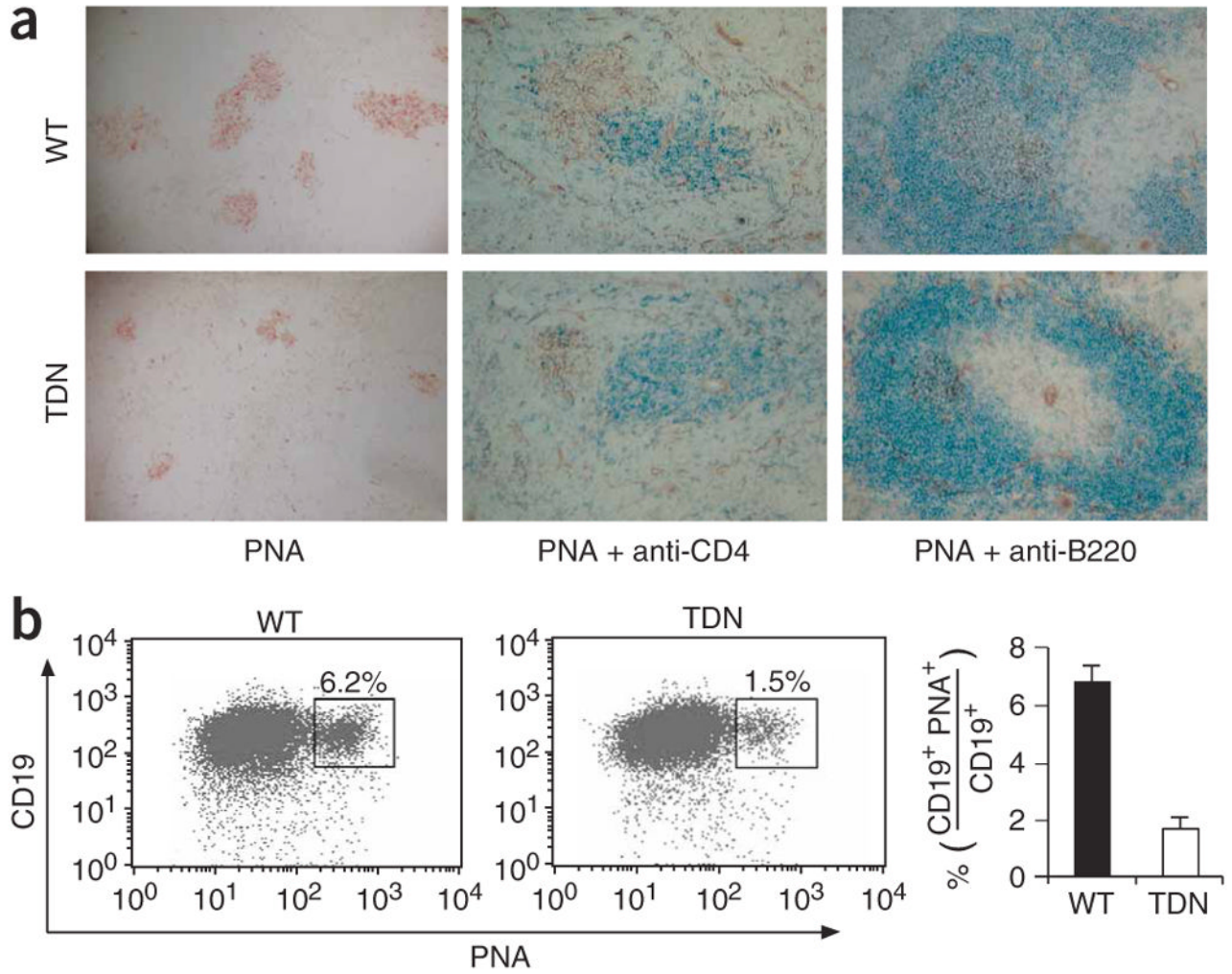


Figure 3. Impaired germinal center formation in TDN-transgenic mice. Nontransgenic mice (WT) and TDN-transgenic mice (TDN) were inoculated intraperitoneally with SRBCs and spleens were collected for analysis. **(a)** Histology for PNA (red; left), PNA (red) plus CD4 (blue; middle), or PNA (red) plus B220 (blue; right). Original magnification, $\times 100$ (left) or $\times 200$ (middle and right). **(b)** Flow cytometry (left) of B220⁺-gated splenocytes. Numbers beside boxed areas indicate percent CD19⁺PNA⁺ cells. Right, proportion of CD19⁺PNA⁺ B cells (expressed as a percent of total CD19⁺ cells), as measured by flow cytometry in three independent experiments (error bars, s.e.m.).

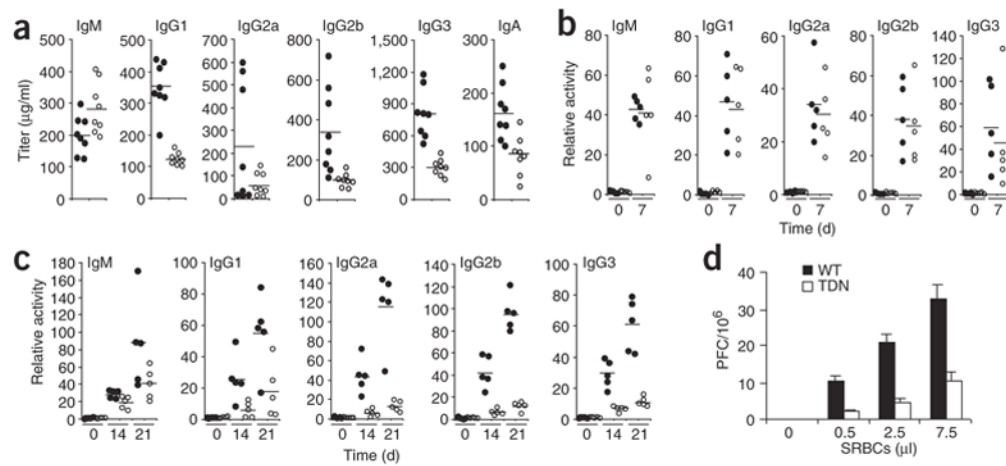


Figure 4.

Impaired T cell-dependent but intact T cell-independent humoral responses in TDN-transgenic mice. **(a)** Immunoglobulin isotype analysis of sera from naive TDN-transgenic mice (open circles) and nontransgenic littermates (filled circles). Each circle represents one mouse. Data are representative of three experiments. **(b,c)** Antigen-specific humoral responses. TDN-transgenic mice (open circles) and wild-type littermates (filled circles) were challenged with the T cell-independent antigen TNP-Ficoll on day 0 **(b)** or the T cell-dependent antigen TNP-KLH on days 0 and 14 **(c)**. Serum collected on days 0 and 7 for T cell-independent responses **(b)** or on days 0, 14 and 21 for T cell-dependent responses **(c)** was assayed for TNP-specific immunoglobulin isotypes; ELISA activity is expressed relative to a titrated standard serum. Data are representative of two independent immunizations. **(d)** Plaque assay for SRBC-specific plasma cells. Splenocytes collected from mice 5 d after challenge with SRBCs were plated in SRBC-containing soft agar and plaque-forming units were counted. Data are expressed as plaque-forming cells per 1×10^6 spleen cells (PFC/ 10^6). Error bars, s.e.m.; $n = 3$ mice per group. Data are representative of two independent experiments.

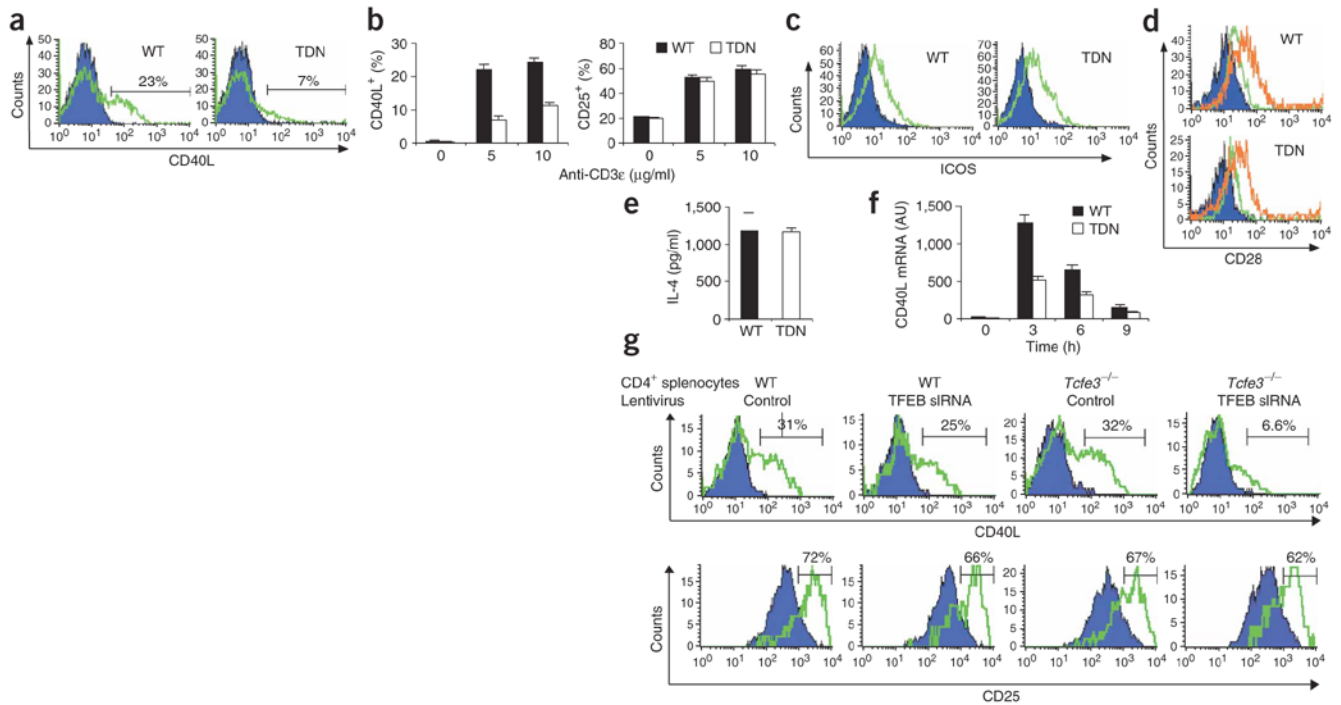


Figure 5. Inactivation of TFE3 and TFEB in CD4 T cells impairs induction of CD40L expression but not the synthesis of other activation and effector molecules. **(a)** Flow cytometry of surface expression of CD40L by control (WT) and TDN-transgenic (TDN) CD4⁺ splenocytes stimulated with mAb to CD3 and analyzed at 8 h. Filled curves, unstimulated cells; green lines, CD3-stimulated cells. Numbers above bracketed lines indicate CD40L⁺ cells. Data are representative of more than three experiments. **(b)** Quantification of histogram data for percent CD4⁺ T cells positive for CD40L (left) and CD25 (right) after 8 h of stimulation with various amounts of mAb to CD3 (Anti-CD3 ϵ). Error bars, s.e.m.; $n = 6$ mice for total CD40L analyses; $n = 3$ mice for analysis of both CD40L and CD25 in the same experiment. **(c,d)** Expression of ICOS **(c)** and CD28 **(d)**. Filled curves, freshly isolated CD4⁺ T cells; green lines **(d)**, cells left unstimulated in culture for 2 d; green lines **(c)** and red lines **(d)**, cells stimulated for 2 d with mAb to CD3. Data are representative of three separate experiments. **(e)** IL-4 secretion. Data are from three independent experiments (error bars, s.e.m.). **(f)** Real-time PCR analysis of RNA isolated from CD4⁺ T cells from wild-type or TDN-transgenic littermate mice at various times after incubation with mAb to CD3 (horizontal axis). AU, arbitrary units. Data are from three independent experiments (error bars, s.e.m.). **(g)** CD40L and CD25 expression by primary CD4⁺ T cells from wild-type and *Tcfe3*^{-/-} mice that were infected with the GFP-only control lentivirus (Control) or TFEB siRNA lentivirus. Filled curves, unstimulated GFP⁺ cells; green lines, TCR-stimulated GFP⁺ cells. Numbers above bracketed lines indicate CD40L⁺ cells (top row) or CD25⁺ cells (bottom row). Data are representative of three independent experiments.

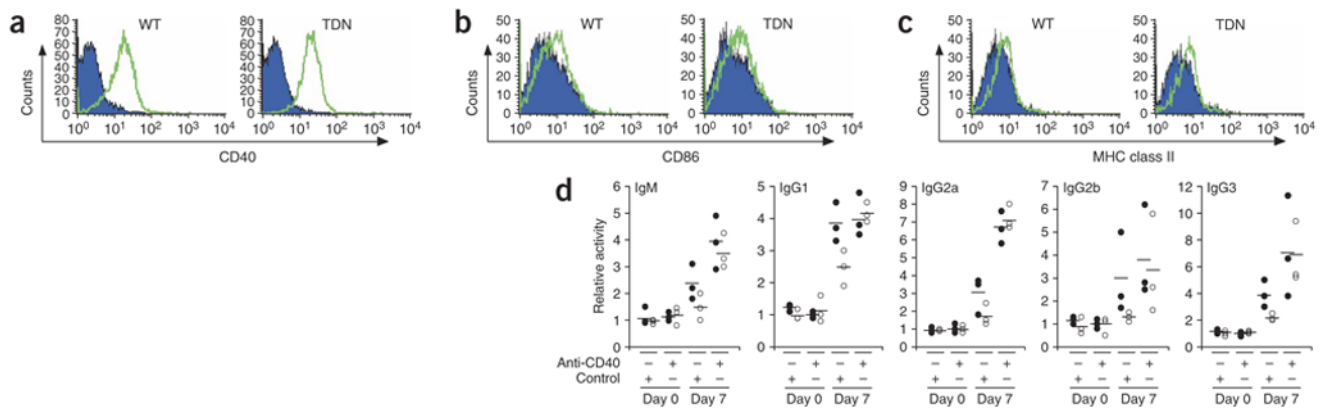


Figure 6.

T cell–dependent IgG responses in TDN-transgenic mice can be restored by CD40 stimulation *in vivo*. **(a)** CD40 expression in B cells from nontransgenic and TDN-transgenic mice. **(b,c)** Expression of CD86 **(b)** and MHC class II **(c)** after stimulation of B cells with mAb to CD40. In **a–c**: filled curves, unstained cells; green lines, cells stained with mAb to CD40. **(d)** IgG responses to TNP-KLH in nontransgenic and TDN-transgenic mice treated with an agonist mAb to CD40 during immunization. Control mice (filled circles) and TDN-transgenic mice (open circles) were immunized intraperitoneally once with 100 μ g TNP-KLH plus 100 μ g of either isotype-matched control antibody (control) or mAb to CD40 (3/23), delivered intravenously. The same amount of each mAb was administered once a day over 7 d. Data represent TNP-specific IgG isotypes from serum samples obtained on days 0 and 7.

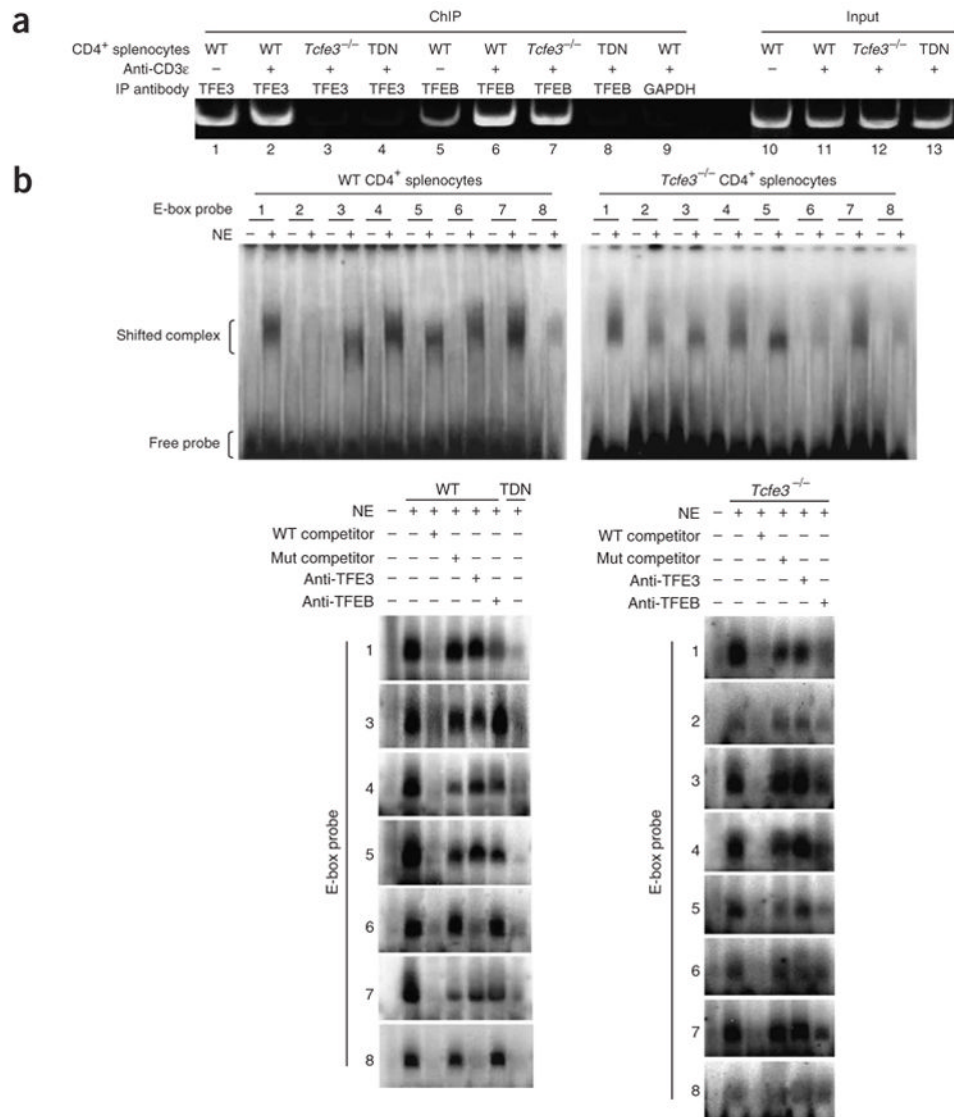


Figure 7. TFE3 and TFEB bind to the *Cd40lg* promoter *in vivo* and *in vitro*. **(a)** Chromatin immunoprecipitation analysis of a *Cd40lg* promoter fragment by TFE3 and TFEB antibodies. Primary CD4⁺ splenocytes from wild-type, *Tcfe3*^{-/-} and TDN-transgenic mice were left unstimulated or were stimulated with mAb to CD3 (above lanes), followed by semiquantitative PCR analysis of 0.11% of the starting material (Input; lanes 10–13) or 10% of the immunoprecipitated material (ChIP; lanes 1–9). Chromatin immunoprecipitation with anti-GAPDH (lane 9) is an additional negative control for background band intensity. Amplification was in the linear range (**Supplementary Fig. 3** and data not shown). Data are representative of three independent experiments. **(b)** Electrophoretic mobility-shift assay to evaluate the binding of native TFE3 and TFEB protein to MiT sites. Nuclear extracts (NE) from stimulated wild-type, *Tcfe3*^{-/-} and TDN-transgenic splenic CD4⁺ T cells were incubated with radiolabeled oligonucleotides spanning a single MiT E-box (sites 1–8; numbered as in **Supplementary Fig. 3**) and complexes were resolved by native gel electrophoresis. Top, relative E-box-binding activity; left margin, shifted complexes and free probe. Bottom, cold oligonucleotide competition and antibody-interference assays to determine the identity and specificity of E-

box-binding complexes in cell extracts. Excess unlabeled E-box oligonucleotides, with wild-type (WT) or with point mutations (Mut), and anti-TFE3 or anti-TFEB were included in some binding reactions (+; above lanes). Bottom exposures were optimized for each probe. Data are representative of at least three independent experiments.

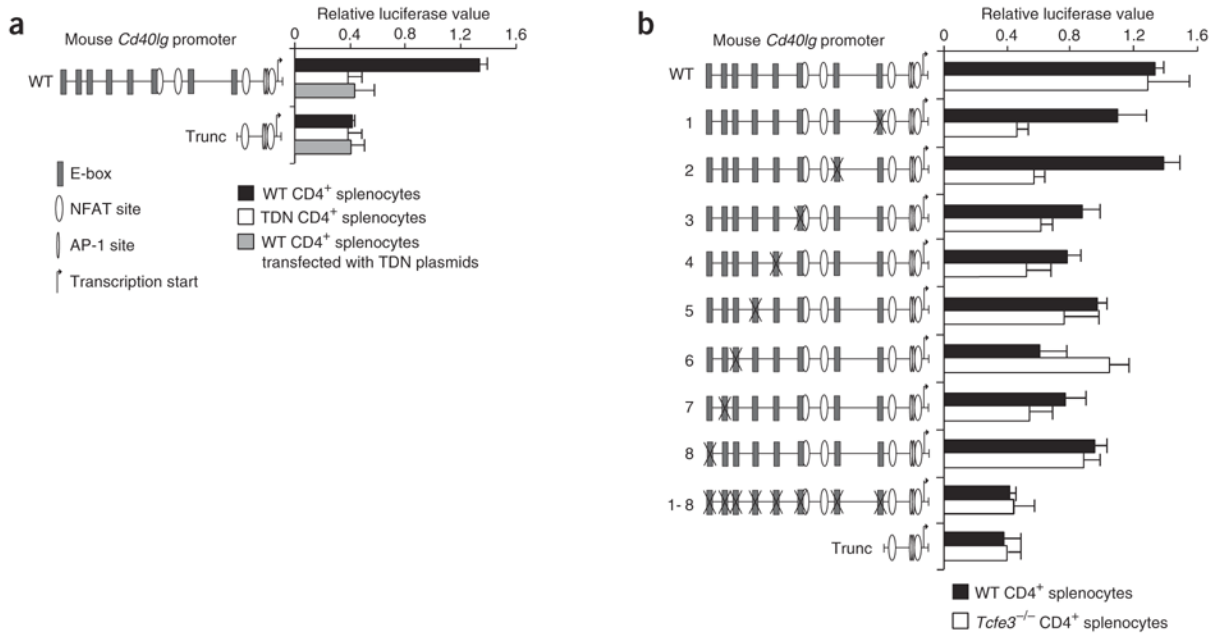


Figure 8.

Maximum *Cd40lg* promoter activity requires binding of native TFE3 and TFEB. **(a)** A *Cd40lg* promoter fragment containing the MiT E-boxes depends on endogenous TFE3 and TFEB to enhance promoter activity. Primary CD4⁺ splenic T cells from wild-type and TDN-transgenic mice were transfected with mouse *Cd40lg* promoter-luciferase constructs, either full-length (from the ATG to -1535 base pairs upstream) or truncated (to -382); RLuc was cotransfected to provide an internal control for normalization. Then, 2 d later, cells were stimulated for 8 h with mAb to CD3, then were collected and lysed for luminometry. Data represent relative luciferase values (normalized to renilla values) of three independent experiments; error bars, s.e.m. ($n =$ three independent transfections using cells prepared from three separate sets of wild-type and TDN-transgenic mice). **(b)** Contributions of individual and combinations of MiT E-box sites to promoter activity. Point mutations abrogating binding of TFE3 and/or TFEB binding ('X') were introduced into E-box sites (numbered 1–8; left margin) in the context of the full-length mouse *Cd40lg* promoter. Primary splenic CD4⁺ T cells from wild-type and *Tcfe3*^{-/-} mice were transfected, stimulated and analyzed for luciferase activity as in described in **a**.